Published in final edited form as:

Nat Immunol. 2016 August ; 17(8): 956–965. doi:10.1038/ni.3514.

Asynchronous combinatorial action of four regulatory factors activates *Bcl11b* for T cell commitment

Hao Yuan Kueh[1,*,5], **Mary A. Yui**[1], **Kenneth K.H. Ng**[1], **Shirley S. Pease**[1], **Jingli A. Zhang**[1,2], **Sagar S. Damle**[1,3], **George Freedman**[1,4], **Sharmayne Siu**[1], **Irwin D. Bernstein**[5], **Michael B. Elowitz**[1,6], and **Ellen V. Rothenberg**[1,*]

[1]Division of Biology and Biological Engineering, California Institute of Technology, Pasadena, CA

[5]Clinical Research Division, Fred Hutchinson Cancer Research Center, Seattle, WA 98109

[6]Howard Hughes Medical Institute, California Institute of Technology, Pasadena, CA 91125

Abstract

During T cell development, multipotent progenitors relinquish competence for other fates and commit to the T cell lineage by turning on the transcription factor Bcl11b. To clarify lineage commitment mechanisms, we followed developing T cells at single-cell level using *Bcl11b* knock-in fluorescent reporter mice. Notch signaling and Notch-activated transcription factors collaborate to activate *Bcl11b* expression, irrespective of Notch-dependent proliferation. These inputs work via three distinct, asynchronous mechanisms: an early locus poising function dependent on TCF-1 and GATA-3; a stochastic permissivity function dependent on Notch signaling; and a separate amplitude-control function dependent on Runx1, a factor already present in multipotent progenitors. Despite all being necessary for *Bcl11b* activation, these inputs act in a stage specific manner, providing a multi-tiered mechanism for developmental gene regulation.

As immune progenitors develop into T cells, they progressively relinquish access to alternative fates and eventually commit to becoming a T cell[1,2]. The final executor of this commitment transition is the *Bcl11b* gene, whose activation is a dramatic lineage-specific landmark in early T cell development. While Bcl11b has many roles in peripheral T cells[3,4], where it is expressed almost universally, its initial activation is essential for establishing T cell identity during development[5]. Deletion of Bcl11b in progenitors blocks T cell commitment[6,7], and also impairs T cell receptor re-arrangements[8] and expansion of β-chain

[*]Corresponding authors: kueh@caltech.edu or kueh@uw.edu, evroth@its.caltech.edu.
[2]Current address: Genentech, 1 DNA Way, South San Francisco, CA 94080
[3]Current address: Department of Bioinformatics, Antisense Drug Discovery, Isis Pharmaceuticals, Carlsbad, CA 92010
[4]Current address: Department of Pediatrics, University of California San Francisco School of Medicine, San Francisco, CA 94143
[5]Current address: Department of Bioenginering, University of Washington, Seattle, Washington, USA (H.Y.K.).

Accession codes. GEO GSE70981: raw sequence reads, normalized expression levels.

Author contributions: H. Y. K. designed research, performed experiments, analyzed data, and wrote the paper. M. A. Y. designed research, performed experiments, analyzed data, and wrote the paper. K.H.K.N., and S. S. P. performed experiments. S. S. D., G. F., and I. D. B. provided reagents. J. A. Z. performed experiments and analyzed data. S. S. analyzed data. M. B. E. designed research. E. V. R. designed research, analyzed data, and wrote the paper.

Competing financial interests notice: The authors report no competing financial interests.

expressing pre-T cells[9]. Later stage deletion can cause mature T cells to become NK-like cells[10].

Bcl11b is activated late in the course of initial T cell specification. Upon stimulation by Notch-Delta signals in the thymus, progenitors first transition from an early T progenitor (ETP) stage, identified as c-Kit$^+$ CD4 and CD8 double-negative (DN)1, to DN2a stage, where Bcl11b expression is first detected at the population level. DN2a progenitors then transition to DN2b stage, where they further increase expression of Bcl11b and lose potential to generate NK or dendritic cells[11,12]. The process of Bcl11b activation and lineage commitment from the earliest thymus-settling post-natal progenitors spans about ten days and cell cycles[13], allowing cells to expand substantially before commitment is complete.

Bcl11b activation and T-lineage commitment depend on Notch signaling, and on an ensemble of transcription factors that includes Runx1, TCF-1 (encoded by *Tcf7*), and GATA-3[14–17]. GATA-3 and TCF-1 are activated by Notch signaling. Runx1, already expressed in hematopoietic stem cells, is also upregulated by Notch[15,18–20]. These factors may all bind the *Bcl11b* locus concurrently to coordinate its activation, following well-established precedents of combinatorial gene regulation[21,22]. In this view, the timing of *Bcl11b* activation would be controlled by slow accumulation of one or more upstream factors, which would need to reach a quorum on the gene locus to cause induction. Alternatively, these factors may collaborate in an asynchronous manner to control Bcl11b expression. Work from several systems has shown that some transcription factors act as `pioneers', and may physically open chromatin around genes to enable subsequent binding of other factors[23,24]. Thus, Bcl11b activation and T lineage commitment could involve the temporally separated action of transcription factors, with some acting early to control activation, and others acting later to maintain expression.

Distinguishing between these models requires isolating cells in distinct gene expression states, and comparing their developmental plasticity. Population-level gene expression measurements, which average over distinct cell states and temporal stages, are not definitive for this. Therefore, to pinpoint the mechanisms of Bcl11b activation and T lineage commitment, we generated a knock-in fluorescent reporter in the *Bcl11b* locus, and followed *Bcl11b* activation dynamics at single-cell level using *in vitro* developmental assays together with flow cytometry and timelapse live imaging. We show that *Bcl11b* activation coincides with commitment at the single-cell level. To activate this locus, multiple transcription factors play precisely staged, often transient roles. The factors controlling *Bcl11b* expression amplitude differ from those that license the locus for expression competence, a regulatory strategy that frees the latter factors to play subsequent roles in mature T cell functional specialization.

Results

Bcl11b-YFP reporter recapitulates Bcl11b expression in T cells

GATA-3, TCF-1, Runx1, and Notch bind to cis-regulatory elements on the *Bcl11b* locus[10,15,25,26] (Supplementary Fig. 1), and all show evidence for functional roles in *Bcl11b* expression[14,16,17,27,28], but how they collaborate to control Bcl11b activation is not

understood. To analyze how Bcl11b activation and T cell lineage commitment work at single-cell level, we generated a knock-in fluorescent reporter mouse strain for *Bcl11b* expression. Using standard gene targeting, we inserted a neomycin-resistant (*neo*) internal ribosome entry site (IRES)-mCitrine (YFP) cassette into the 3'-untranslated region (UTR) of *Bcl11b* in mouse embryonic stem (ES) cells (Fig. 1a, Supplementary Fig. 2a). We then injected correctly targeted ES cells into blastocyst-stage embryos to generate *Bcl11b*$^{+/YFP}$ mice. This knock-in reporter recapitulated the dynamic regulation of *Bcl11b* in adult T cell progenitors. Bcl11b was silent in c-Kit^{hi} DN1 thymocytes (ETPs), and began to be expressed in DN2a thymocytes (Fig. 1a, top), as previously observed[11,25,29]. DN2a progenitors comprised two distinct populations, one where Bcl11b-YFP expression was not yet detectable, and another showing clear expression (Fig. 1a), suggesting that Bcl11b activation occurs after transition to the DN2a stage. Bcl11b-YFP expression increased during DN2b and DN3 stages, i.e. to TCRβ rearrangement, and was stably maintained in all subsequent stages and major effector T cell subsets, but not detected in B and NK cells (Fig. 1b). *Bcl11b*$^{YFP/YFP}$ T cells had approximately two-fold higher YFP expression than *Bcl11b*$^{YFP/+}$ cells, for all subsets analyzed (Fig. 1ab). Together with the unimodal YFP expression in Bcl11b$^{YFP/+}$ T cells beyond DN2a stage, this finding indicated that both Bcl11b alleles were activated in the large majority of T cells. Mice with the *neo*-containing Bcl11b-YFP knock-in allele were used in all experiments shown here, but importantly, *neo* cassette excision from the Bcl11b-YFP locus did not affect its expression pattern (Supplementary Figure 3).

Bcl11b turns on after DN2a stage entry

Previous analysis of Bcl11b expression has indicated that ETPs first differentiate into CD25^{+} DN2a thymocytes, then turn on Bcl11b expression, and finally down-regulate CD44 and c-Kit to enter the DN2b and DN3 stages. To directly verify this developmental sequence, we sorted ETP, Bcl11b-YFP^{-}DN2a and Bcl11b-YFP^{+}DN2a and (uniformly) Bcl11b-YFP^{+}DN2b thymocytes, and analyzed their developmental progression on OP9-DL1 stromal cell monolayers, an *in vitro* system that recapitulates all early stages of T cell development[30]. After three days, ETPs activated Bcl11b, but only after becoming CD25^{+} (Fig. 1c). The majority of Bcl11b-YFP^{-} DN2a cells turned on Bcl11b and a subset of those down-regulated expression of CD44, indicating a transition to the DN2b and DN3 stages (Fig. 1c). Thus, Bcl11b activation is a discrete regulatory event that occurs after transition into the DN2a stage.

Bcl11b activation coincides with T lineage commitment

Transition of developing thymocytes from DN2a to DN2b stages coincides with loss of alternate lineage potential and commitment to the T lineage[11]. Loss of alternative potential could occur upon Bcl11b activation in DN2a thymocytes or only after transition of Bcl11b^{+} DN2a cells to the DN2b stage. To distinguish between these possibilities we isolated (Bcl11b-YFP^{-}) ETP, Bcl11b-YFP^{-} DN2a, Bcl11b-YFP^{+} DN2a and (Bcl11b-YFP^{+}) DN2b progenitors from the thymi of wild-type mice, then compared their NK cell and DC potentials by culturing them on OP9 stromal cells that do not stimulate Notch-Delta signaling (Fig. 2a; see Methods for stromal cell nomenclature). When 300 sorted cells of each subset were cultured in these conditions, Bcl11b-YFP^{-} ETP and Bcl11b-YFP^{-} DN2a thymocytes maintained the potential to differentiate into NK cells and DCs, consistent with

previous observations, while NK and DC potential dropped sharply in Bcl11b-YFP^{+}DN2a cells, and was absent in DN2b thymocytes (Fig. 2a). This finding was confirmed in limiting dilution cell cultures (Fig. 2a, lower panels). These results indicate that Bcl11b-YFP^{+} DN2a cells are already more restricted than Bcl11b-YFP^{-}DN2a cells in alternative developmental potentials.

Molecular context and signature of Bcl11b activation

To determine the genome-wide transcriptome changes that accompany the change in developmental potential that accompanies Bcl11b activation, we carried out RNA-seq gene expression analysis using culture of immature bone marrow cells on OP9-DL1 monolayers as a source of large numbers of semi-synchronized DN thymocytes (Fig. 2b). Cells were sorted after a week in culture, when the majority of cultured CD45^{+} cells were DN2 cells just beginning to turn on Bcl11b, with a minority remaining c-Kit^{+}CD44^{+} CD25^{-} ETP-like (henceforth called ETP)(for *ex vivo* and *in vitro*-derived population criteria, see Methods). Similar to thymic progenitors, bone marrow-derived progenitors showed a reduction in NK cell potential upon Bcl11b activation (Fig. 2c). Transcriptome analysis showed that the patterns of gene expression in bone marrow-derived DN2 subsets first turning on Bcl11b-YFP fell into a smooth trajectory in principal component space, which was intermediate between early DN2a cells and DN2b cells (Fig. 2d). Heat maps of gene expression for the most dynamically changing genes overall (Fig. 2e, Supplementary Table 1) and for functionally important transcription factor genes (Fig. 2e, Supplementary Table 2a) are also shown. As DN2 cells progressed from Bcl11b-YFP^{-} to Bcl-11b-YFP^{+}, they increased expression of T cell identity genes, including T cell receptor signaling components (*Cd3g, Cd3d, Lat*) and the recombinase activating gene *Rag1* (Fig. 2e, gold), while downregulating stem cell-, NK cell- and myeloid cell-associated genes (Fig. 2e, blue, green and black), consistent with their reduced lineage plasticity. Known T cell developmental regulators showed very limited expression changes as Bcl11b-YFP expression was turned on (Fig. 2e). Multiple differences were observed between ETP and Bcl11b-YFP^{-} DN2 progenitors (*Ets1, Tcf7, Dtx1, Bcl11a, Sfpi1, Mef2c and Lmo2*, $p < 0.005$; Supplementary Table 2a,b), and between Bcl11b-YFP^{lo} and Bcl11b-YFP^{+} DN2 cells (*Sox13, Ets1, Lmo2*, $p < 0.005$; Supplementary Table 2a,b). However, for the same probability cutoff, no significant expression differences among regulators could be observed between Bcl11b-YFP^{-} and Bcl11b-YFP^{lo} cells, except for Bcl11b itself (Supplementary Table 2b). Gene expression and lineage potential assays together thus demonstrate that Bcl11b activation in individual cells coincides with loss of lineage plasticity and acquisition of a committed T cell state.

Control of Bcl11b activation by Notch and IL-7 signaling

Bcl11b is expressed only in the Notch-driven T cell and innate lymphoid cell 2 programs (ILC2) (rev. in[31]), and chromatin immune precipitation evidence shows binding of Notch1 intracellular domain and CSL to the Bcl11b locus (Supplementary Fig. 1),[10,26] suggesting that Notch-Delta signaling may regulate Bcl11b expression directly. Bcl11b activation may also be triggered by removal of IL-7-IL-7R signals[7]. We therefore examined how Notch signals and IL-7 withdrawal affected *Bcl11b* activation in individual bone marrow-derived DN progenitors, sorted from OP9-DL1 pre-cultures at different stages of development. Like ETP thymocytes, bone marrow-derived progenitors cultured with Notch ligands and IL-7

turn on CD25 to enter the DN2a stage, and then turn on Bcl11b to enter a committed state (Fig. 3a).

Optimal Bcl11b-YFP induction from input BM-derived ETPs depended on Notch signaling and on minimizing IL-7 amounts in culture (Fig. 3b), consistent with previous reports[7]. ETPs activated Bcl11b-YFP much more efficiently when growing on OP9-DL1 than on OP9, and most efficiently on OP9-DL1 when IL-7 was removed (Fig. 3b). ETP cells cultured on OP9 stroma down-regulated the stem cell marker c-Kit (Fig. 3b, left), consistent with differentiation into an alternate lineage. However, for cells that had already activated Bcl11b-YFP, Notch signaling was unnecessary for maintaining Bcl11b expression (Fig. 3b). Bcl11b-YFP$^+$ cells maintained similarly high Bcl11b-YFP expression after four days of culture on OP9 and OP9-DL1 stromal cells alike, even though CD25 expression was strongly downregulated in the same Bcl11b-YFP$^+$ cells on OP9 compared to OP9-DL1 cultures (Fig. 3b). Similarly, IL-7 dosage in the culture had little effect on maintenance of Bcl11b-YFP expression by Bcl11b-YFP$^+$ cells (Fig. 3b). Between these poles, in Bcl11b-YFP$^-$ DN2 cells IL-7 withdrawal also caused a moderate increase in Bcl11b-YFP$^+$ frequency, while accelerating the down-regulation of c-Kit (Fig. 3b). However, unlike ETP cells, Bcl11b-YFP$^-$ DN2 cells cultured on OP9 showed a split response after four days (Fig. 3b, middle columns). About 50% of the Bcl11b-YFP$^-$ DN2 cells on OP9 failed to up-regulate Bcl11b-YFP, but 50% activated Bcl11b-YFP at least as robustly as on OP9-DL1 (Fig. 3b). These results suggest that Notch signaling and IL-7 mainly affect onset, not maintenance of Bcl11b expression.

Bcl11b-YFP activation is independent of the cell cycle

The results could indicate that Notch signaling activates Bcl11b-YFP expression or that it selectively promotes proliferation of Bcl11b-YFP$^+$ cells. To distinguish these options, we measured cell division rates of Bcl11b-YFP$^-$ DN2 progeny using CellTrace Violet. Bcl11b-YFP$^-$ DN2 cells cultured on OP9-DL1 went through 8 cell cycles of cell division in 4 days compared to 5–6 cell cycles on OP9 in the same time interval (Fig. 4a,b). However, poised progenitors that turned on Bcl11b-YFP divided a similar number of times as those remaining Bcl11b-YFP negative, whether cultured on OP9 or OP9-DL1 (Fig. 4a). Thus, Notch signaling did not expand Bcl11b-expressing cells preferentially.

Still, Notch signaling effects on proliferation raised the possibility that *Bcl11b* activation could require passage through a threshold number of cell cycles, and this could bias detection of *Bcl11b* transcription in favor of Notch-signaled cells. Such a cell-cycle counting mechanism could be based on a need to remodel chromatin during S phase, to reposition it after mitosis or to dilute out pre-existing negative regulators, and could involve the Notch-induced cell cycle driver c-Myc[32]. We therefore tested whether the effect of Notch signaling on Bcl11b-YFP activation in Bcl11b-YFP$^-$ DN2 cells was altered by over-expression of Myc, which accelerates proliferation, or by treatment with the cyclin-dependent kinase inhibitor PD0332991, which slows proliferation[33]. Bcl11b-YFP$^-$ DN2 cells retrovirally transduced with Myc proliferated as much in OP9 cultures as in OP9-DL1 cultures (Fig. 4b). However, Myc over-expression had little impact on Bcl11b activation compared to empty vector in the cells in OP9 co-culture (Fig. 4c). Conversely, PD0332991 severely blocked

proliferation (Fig. 4b), but did not significantly impede Bcl11b activation by Bcl11b-YFP$^-$ DN2 cells (Fig. 4c) compared to untreated controls. Thus, a cell cycle counting-based mechanism is not rate-limiting for *Bcl11b* induction in Bcl11b-YFP$^-$ DN2 cells. Together, these results suggest that Notch signaling directly enhances Bcl11b activation rate, independent of the cell cycle.

Notch signals enhance probabilistic rate of *Bcl11b* induction

To directly visualize effects of Notch on poised Bcl11b-YFP$^-$ DN2 progenitors, we sorted Bcl11b-YFP$^-$ DN2 cells derived from bone marrow precursors, and re-cultured them on OP9 and OP9-DL1 stroma with continuous live imaging. When cultured on OP9 stroma, a small fraction of cells turned on Bcl11b-YFP expression within the first two days of imaging observation (Fig. 5a,b), and this fraction increased steadily until it reached a plateau value of ~0.4 at about 80–90 hours of culture(Fig. 5c–e). Compared to OP9 stromal cultures, OP9-DL1 stroma doubled the fraction of cells that turned on Bcl11b-YFP expression even at <2 days of culture (Fig. 5a,c,d, e) and accelerated first Bcl11b-YFP induction for individual cell lineages, as assessed by single-cell tracking (Fig. 5b). This indicates that Notch signaling plays a direct and immediate role in controlling Bcl11b activation. Even with continued Notch signaling, the fraction of cells expressing Bcl11b also appeared to reach a plateau value (~0.8, Fig. 5e), suggesting that DN2 progenitors that do not initiate Bcl11b-YFP expression may eventually lose the ability to activate this gene, although this possibility will require further investigation. Thus, while Notch signaling is not strictly necessary for *Bcl11b* transcriptional activation, it enhances the probabilistic rate of this event.

To assess how much Notch signaling is needed for Bcl11b activation, we compared the dose-dependence of Bcl11b transcriptional activation on Notch signaling to the threshold for two other Notch-dependent responses, CD25 upregulation and restriction of non-T lineage development. Bcl11b-YFP$^-$ DN2a thymocytes were cultured in stromal cell-free conditions for 4 days with a range of doses of purified DL1-Fc (0–3.2 μg/ml) pre-bound to tissue culture plates[34]. DL1-Fc increased the fraction of DN2a cells becoming Bcl11b-YFP$^+$ in a dose-dependent manner, but even a low dose of 0.2 μg/ml DL1-Fc enabled 50% the cells to turn on Bcl11b-YFP (Fig. 6a). Furthermore, increasing DL1-Fc concentrations enhanced the frequency of cells becoming Bcl11b-YFP$^+$, but not the expression magnitudes of Bcl11b-YFP in individual positive cells (Fig. 6; cf. bimodal response in Fig. 3b). Similar dose-effects were observed upon pharmacological inhibition of Notch signaling by γ-secretase Inhibitor (Supplementary Fig. 5). Bcl11b-YFP could be fully activated in a major subset of DN2 cells by culture with DL1-Fc concentrations that did not sustain CD25 expression and did not suppress trans-differentiation to CD11c$^+$ dendritic cells (Fig. 6b). Thus, Bcl11b activation requires a lower Notch signal compared to that required to regulate these other processes.

GATA-3 and TCF-1 control poising of *Bcl11b* for activation

The lower threshold for Notch signals to induce Bcl11b-YFP in DN2a thymocytes compared to ETPs suggested that another rate-limiting factor collaborates with Notch at DN2a stage to promote Bcl11b-YFP activation. Such factors could be activated by Notch signaling before or coincident with Bcl11b-YFP activation. Our transcriptome analyses showed few if any

new regulatory gene candidates to increase expression between Bcl11b-YFP^{-} DN2 and Bcl11b-YFP^{lo} DN2 besides *Bcl11b* itself (Fig. 2f; Supplementary Table 2b), although their activity or expression could be modulated post-transcriptionally. Therefore, we examined the roles of T cell transcription factors implicated previously by genetic evidence, namely GATA-3, TCF-1 (encoded by *Tcf7*) and Runx factors in a complex with CBFβ.

The T-cell specific factors GATA-3 and TCF-1 are activated by Notch signaling in the ETP stage, before Bcl11b activation[35,36]. To determine how and when these factors are needed for Bcl11b expression, we knocked down their expression in progenitors at different developmental stages using shRNA constructs, all validated in ETP and DN2 cells (Supplementary Fig. 6)[17]. Transduction of shRNA-*Gata3* and shRNA-*Tcf7* into ETP cells severely inhibited induction of Bcl11b-YFP in their progeny compared to cells transduced with a non-targeting control (shRandom)(Fig. 7a). GATA-3 and TCF-1 knockdown in descendants of DN1 cells mainly reduced the percentages of cells expressing Bcl11b-YFP, rather than the amount of Bcl11b-YFP expressed per cell (Fig.7a), like the effects of Notch inhibition. Production of CD25^{+} cells was also severely affected as expected[15,16,19], consistent with an early developmental block. Although some of the cells did acquire a DN2 phenotype, shRNA-*Tcf7* further reduced the fraction of DN2 cells that activated Bcl11b-YFP.

However, transduction of either shRNA-*Gata3* or shRNA-*Tcf7* into Bcl11b-YFP^{-} DN2a cells had much less effect on Bcl11b-YFP activation than in ETPs (Fig. 7ab). Knockdown of GATA-3 from DN2a stage on had no detectable effects on Bcl11b-YFP activation. In DN2a cells, shRNA-*Tcf7* effectively lowered a barrier to DC trans-differentiation (Supplementary Fig. 7a) but only mildly impeded Bcl11b-YFP induction compared to shRandom vector controls (Fig. 7ab). By DN2b stage, knock down of TCF-1 or GATA-3 had no effect on Bcl11b-YFP expression compared to random shRNA (Fig. 7b; Supplementary Fig. 8), consistent with reported RNA expression data[37,38]. Conversely, TCF-1 over-expression did not affect Bcl11b-YFP expression in either ETP or DN2 cells in our system (Supplementary Fig. 7b), suggesting that physiological levels of TCF-1 protein at ETP or DN2 stage are sufficient for maximum Bcl11b induction. These results indicate that GATA-3 and TCF-1 together control entry of cells into a state poised for Bcl11b activation, but are largely dispensable for maintaining Bcl11b expression after commitment.

Runx1 controls Bcl11b expression amplitude

We next investigated how Bcl11b expression amplitude is controlled once activated. Because Runx-CBFβ transcriptional complexes are vital for development of T cells past the DN2 stage[14,39], Runx binding sites are prominent in the cis-regulatory regions of *Bcl11b*[27], and germline CBFβ dose reduction severely impacts *Bcl11b* expression[14], we tested whether Runx has a role in regulating *Bcl11b* transcription. We transduced Bcl11b-YFP^{-} DN2 (Fig. 8a) or Bcl11b-YFP^{+} (Fig. 8b) DN2 progenitors with either a Runx1 shRNA or a pan Runx dominant negative (Runx-DN) construct[40] to inhibit Runx activity, or with full length Runx1 cDNA to elevate Runx1 activity, and assessed the impacts on the magnitude of Bcl11b-YFP expression. shRNA-*Runx1* down-shifted the whole distribution of Bcl11b-YFP expression compared to random shRNA or empty vector, whereas Runx1 over-expression up-shifted

Bcl11b-YFP expression, both during Bcl11b-YFP induction (Fig. 8a) and in cells that were already Bcl11b-YFP$^+$ (Fig. 8b). Pan Runx-DN had a similar but milder effect than shRNA-Runx1 in both cell types, suggesting that other Runx family members may only play minor roles. shRNA-*Runx1* transduction also affected Bcl11b-YFP expression in descendants of both Bcl11b-YFP$^-$ DN2 (Fig. 8a) and Bcl11b-YFP$^+$ DN2 cells (Fig. 8b) in the absence of Notch signaling (OP9, right panels), indicating that Runx supports the Notch-independent phase of Bcl11b expression as well.

To determine whether the roles established for Runx1, TCF-1 and GATA-3 during commitment persist, we examined their effects on Bcl11b expression in mature T cells. Knockdown of Runx1, but not TCF-1 or GATA-3, in activated, mature peripheral T cells reduced Bcl11b-YFP expression compared to control-transduced cells, both in CD8$^+$ (Fig. 8f,g) and in CD8$^-$ T cells (Supplementary Fig. 8). These data show that Runx1 plays a role distinct from that of Notch, GATA-3, or TCF-1, and controls the magnitude of Bcl11b expression even after T cells leave the thymus.

DISCUSSION

Bcl11b is induced sharply from a silent, repressed state to become fully expressed during commitment, between DN2a and DN2b stages. Although further modulated according to effector lineage and activation state[3,4], Bcl11b is permanently expressed in all T cells, where it upholds T cell identity and suppresses NK fate[3,5]. Here we used a fluorescent *Bcl11b* reporter allele to show that the silence of *Bcl11b* in early ETPs is functionally different from its poised quiescence in early DN2a cells, before it activates dramatically during the T lineage commitment transition. We show that Notch signaling, GATA-3, TCF-1, and Runx1 play distinct, stage-specific roles in controlling this watershed regulatory event. Notch-Delta signaling enhances the likelihood of switch-like Bcl11b activation from “poised” progenitors, but is dispensable to sustain Bcl11b expression once activated. GATA-3 and TCF-1 control entry into a state poised for Bcl11b activation, but are also unnecessary for stable expression of Bcl11b. Thus, Notch, GATA-3 and TCF-1 primarily act permissively. Notably, both GATA-3 and TCF-1 are activated by Notch signaling, suggesting a double feed-forward network circuit architecture for commitment control. In contrast, Runx1 continuously affects Bcl11b expression magnitude with or without Notch signals, indicating an independent role in controlling Bcl11b expression after locus activation. Thus, multiple transcription factors, all necessary for T cell generation, collaborate asynchronously to establish cellular identity, and single-cell tracking clearly distinguishes the mechanisms they use to poise cells for commitment from those to execute and maintain lineage-specific gene expression.

Collaboration of multiple transcription factors is fundamental for establishing distinct cell type identities during multicellular organismal development[41], and is also essential for artificial cell fate reprogramming[42,43]. In classical models of developmental gene regulation, it is often assumed that combinatorial function reflects synchronous transcription factor action at *cis*-regulatory DNA elements of target genes[21,22]. However, it is not clear whether all co-occupancy reflects synchronous transcription factor function. In a growing number of systems, lineage-specifying transcription factors are seen to act as `pioneers’, binding early

to physically open up developmental gene loci and enable subsequent binding of other factors[23,24]. These pioneer factors need not work coordinately with other factors, and may act transiently to generate lasting effects on gene expression[23].

Our results suggest that GATA-3 and TCF-1, which turn on early in ETP cells, may act to "poise" Bcl11b for activation at a later stage. Once the Bcl11b locus is poised in Bcl11b-YFP$^-$ DN2 cells, it then transitions to an active state in a Notch-dependent, IL-7-restrained manner, and then sustains expression through active regulation by Runx1. In this model, the combinatorial requirement for Notch, GATA-3 and TCF-1 makes Bcl11b induction possible only along a narrow range of developmental tracks: the T cell program and the ILC2 program[31]. By the time cells reach Bcl11b-YFP$^-$ DN2 stage, they harbor a potential for activating Bcl11b that ETP cells lack, being "licensed" for Bcl11b activation. This licensing function could be highly related to "pioneering" or locus opening[23,24]; and is distinctive in that individual mediators of licensing can be removed later without affecting expression. An alternative interpretation is that GATA-3 and TCF-1 regulate Bcl11b indirectly through a later-acting intermediate factor, but the paucity of major regulatory changes concomitant with Bcl11b activation disfavors this possibility. When the Bcl11b locus is licensed for activation in "poised" cells (Bcl11b-YFP$^-$ DN2), activation still takes 2–4 days; these remarkably slow kinetics could involve a rate-limiting transition of the locus from an inactive to an active chromatin state, potentially through slow removal of repressive histone marks, DNA demethylation or translocation of the gene locus from the nuclear lamina[25,27], an idea we are currently investigating. Once the Bcl11b locus is activated, its magnitude of expression is sustained by Runx factors. Although Runx factors are expressed from a much earlier stage, they may not be able to reach the relevant sites in the Bcl11b gene until after the "licensing" process is complete, possibly due to the initially repressed state of the *Bcl11b* locus[27].

Unlike lessons gleaned from other well-studied genes, the mechanisms controlling the competence of *Bcl11b* to be turned on are thus distinct from those controlling its expression levels. This distinction is only revealed at the single-cell level. The hit-and-run licensing functions performed by Notch, GATA-3, and TCF-1 are separable from the continuous magnitude control by Runx1. We speculate that this separation is a key to potential developmental importance. The same factors that work together to create the T cell identity in progenitors end up working divergently in later effector T cell subsets. All of these cells need Bcl11b – but Notch signaling is shut down in most naive T cells; and TCF-1 and GATA-3 work together to control T_H2 differentiation in CD4$^+$ T cells, but the TCF-1/GATA-3 ratio is tipped one way in CD8$^+$ T effector cells and in the opposite way in regulatory T cells. We propose that these cells all continue to express Bcl11b because they express Runx1 or other Runx family members, and also share the developmental history of passing through the lineage-specific licensing process studied here. Making locus opening difficult but irreversible, using different factors to modulate levels, provides T cells with a guarantee that these factors can be re-used in multiple contexts. Given that transcription factors are typically re-deployed multiple times in multicellular organism development, we speculate that similar types of mechanisms might underlie regulation in other systems not yet studied in this way.

ONLINE METHODS

Constructs

Gene targeting vectors for reporter insertion into *Bcl11b* were generated using a bacterial artificial chromosome (BAC) recombineering method[44], involving two major steps. Firstly, a modified BAC containing the fluorescent reporter to be inserted into Bcl11b locus was generated. An internal ribosome entry site (IRES)-histone 2B-mCitrine yellow fluorescent protein (YFP) cassette was joined to a loxP-flanked kanamycin/neomycin (neo) drug selection cassette using fusion PCR, and inserted into a cloning vector (pGEM-T Easy, Promega, Madison, WI). Additional 5' and 3' homology arms to the 3'-untranslated region (UTR) of Bcl11b were then attached to this IRES-YFP-neo cassette through an additional round of fusion PCR. The resultant linear fragment was then inserted into a BAC containing the entire Bcl11b gene locus (RP24-282D6, from http://bacpac.chori.org), using a recombineering-competent bacterial strain (SW102,[44]). Correctly targeted BACs were then selected using kanamycin, and verified using PCR and pulse-field gel electrophoresis.

Secondly, targeting sequence from the reporter-modified BAC was retrieved. To generate a retrieval vector, homology regions for the ends of the short and long arms of the targeting vector were joined by fusion PCR, and ligated into a starting ampicillin-resistant vector (PL253,[44]) using the restriction enzymes NotI and SpeI (New England Biolabs, Ipswich, MA). Targeting sequence from the modified BAC was then retrieved into this vector using recombineering in SW102 cells, and resultant targeting vectors were selected using kanamycin and ampicillin. In performing this reaction, it was discovered that a 430bp sequence in the starting PL253 vector (between the restriction enzymes NotI and DraIII) recombined with the fluorescent protein cassette to generate an undesired side-product; this region was removed by excision using NotI and DraIII, followed by ligation using a bridging oligonucleotide containing these adjacent sites for these two restriction enzymes.

Banshee retroviral constructs were used as a starting point for constructing shRNA knockdown vectors[17]. To minimize interference in detection of Bcl11b-YFP fluorescence, we first made a mCherry-expressing shRNA retroviral backbone (Banshee-mCherry), by modifying the existing GFP-based shRNA knockdown vector (Banshee-GFP) using PCR cloning[45]. shRNA targeting sequences for Tcf7, Gata3, Runx1, or a random sequence, were then joined to a U6 promoter by oligonucleotide synthesis, and cloned into this Banshee-mCherry backbone using the restriction enzymes BglII and HindIII. Hairpin sequences for these vectors are provided in Table S1.

Retroviral over-expression constructs were made from an mCherry-expressing backbone we previously generated (MSCV-IRES-mCherry)[33], which was based on the NGFR derivative of the pMIGR1 retroviral vector kindly provided by L. Xu and W. Pear. Full length Runx1 and the Runx dominant negative constructs were made in the laboratory by J. Telfer[46], and were cloned upstream of the IRES sequence of this vector using the restriction enzymes BglII and EcoRI. The Histone-2B mCherry construct was inserted into the MSCV-NGFR vector using PCR cloning with the restriction enzymes BglII and EcoRI. All constructs were verified by sequencing. TCF-1 over-expression constructs and corresponding empty vector controls (MSCV-VEX-GFP) were kindly provided by A. Bhandoola.

To generate non-fluorescent OP9-DL1 cells for live-cell imaging, we generated a pMX-DL1-IRES-hCD8 retroviral construct for transfection into OP9 cells. This was achieved by PCR cloning of mouse Delta-like 1 from a cDNA clone (GenBank BC057400) into the pMX-IRES-hCD8 backbone (gift from N. Masuyama) using the restriction enzyme XhoI.

Generation of Bcl11b-YFP knock-in reporter mice

The IRES-YFP-neo cassette was knocked into the endogenous Bcl11b locus of V6.5 ES cells, through gene targeting vector transfection, followed by selection of individual neomycin/G418 resistant clones. Correctly targeted clones were identified by PCR and Southern Blot analysis (Fig. S2) and injected into C57/BL6 blastocyst embryos. Chimeric founder animals were then crossed to C57/BL6 mice, and offspring containing the knock-in reporter were then bred to homozygosity for this allele. To delete the loxP-flanked neomycin cassette from this reporter allele, Bcl11b animals were bred to the EIIA-Cre mouse strain [B6.FVB-Tg(EIIa-cre)C5379Lmgd/J, from Jackson labs], which expresses Cre recombinase in the germline. Offspring with a deleted neomycin cassette were identified using PCR, and then bred to homozygosity for this allele. For *in vitro* assays with bone marrow progenitors, Bcl11b-YFP mice were crossed to Bcl2 transgenic mice [B6.Cg-Tg(BCL2)25Wehi/J, from Jackson labs] to obtain offspring heterozygous for both alleles; the Bcl2 transgene was used to enhance cell survival in these assays. As V6.5 ES cells represent a hybrid between C57/BL6 and 129/Sv strains, we estimate that mice used for our experiments have a small (< 12.5%) contribution from the 129/Sv genome. Both male and female animals were used as cell sources as we did not observe and sex-specific differences in our experimental results. Spleen and thymus were harvested from 4–6 week old mice, whereas bone marrow was harvested from 2–3 month old mice. All animals were bred and maintained in the Caltech Laboratory Animal Facility, under specific pathogen free conditions, and the protocol supporting animal breeding for this work was reviewed and approved by the Institute Animal Care and Use Committee of the California Institute of Technology.

Analysis of cell populations from thymus and spleen

To analyze Bcl11b-YFP expression in different cell populations, mice were sacrificed, thymuses or spleen were dissected, and single-cell suspensions were made. For later-stage precursors (ISP, DP, CD4, CD8 in the thymus), and for mature populations (CD8, CD4, CD4+CD25+, γδT, NKT, B, NK in the spleen), thymocyte or splenocyte cell suspensions were directly stained using antibodies to cell surface markers (Supplementary Table 4), and analyzed using a benchtop flow cytometer (MacsQuant, Miltenyi). For earlier stage precursors (ETP, DN2a, DN2b, DN3, DN4), mature cells were depleted from thymocyte suspensions by staining with biotinylated antibodies to mature cell markers and removal with streptavidin-conjugated magnetic beads before staining with fluorochrome-conjugated antibodies, as previously described[11]. Antibodies used for this analysis are all standard, commercially available monoclonal reagents with widely-established use to characterize immune cell populations in the mouse; details are given in Supplementary Table 4.

In vitro generation of T-cell progenitors from bone marrow

DN T-cell progenitors were obtained through *ex vivo* expansion of bone marrow stem and progenitor cells on OP9-DL1 co-cultures, following previously described procedures[17,20,47]

with minor modifications. Briefly, bone marrow was removed from the femur and tibia of 2–3 month old Bcl11b-YFP mice. Suspensions of bone marrow cells were then prepared, stained for lineage markers using biotin-conjugated lineage antibodies (CD11b, CD11c, Gr1, TER-119, NK1.1, CD19, CD3), incubated with streptavidin-coated magnetic beads (Miltenyi Biotec), and passed through a magnetic column (Miltenyi Biotec). Lineage-depleted (Lin-) cells were eluted and stored in liquid nitrogen in freezing media (50% FBS, 40% αMEM, 10% DMSO) for future use. To facilitate their development into the DN2 stage, frozen bone marrow cells were thawed and cultured on OP9-DL1 monolayers[30] using standard culture medium [80% αMEM (Gibco), 20% HyClone Fetal Bovine Serum (Thermo Scientific), Pen Strep Glutamine (Gibco), 50 μM β-Mercaptoethanol (Sigma)] supplemented with 5 ng/ml IL-7 and 5 ng/ml Flt3L (Peprotech). To isolate T-cell progenitors, cultured cells were directly sorted after 7 days, or transduced with retroviral constructs 1 day prior to sorting. T-cell precursor subsets were sorted from the cultures using c-Kit, CD44, and CD25 to approximate as closely as possible ETP, DN2a, and DN2b phenotypes found in thymus. However, because the levels of c-Kit expression on these cultured T-cell precursors do not split populations as sharply as those found in vivo, we refer to these bone-marrow derived subsets as ETP, Bcl11b-YFP^{neg} DN2, and Bcl11b-YFP^{+} DN2, respectively.

For retroviral transduction, cultured cells were disaggregated, filtered through a 40 μm nylon mesh, transferred onto Retronectin/DL1-coated virus bound plates prepared as described below, and cultured with standard media supplemented with 5 ng/ml IL-7, 5 ng/ml Flt3L, and 5 ng/ml SCF. For sorting, cells were stained with CD45, CD44, c-Kit, CD25, and a biotin-conjugated lineage cocktail (CD11b, CD11c, Gr1, TER-119, NK1.1, CD19, CD3), (for some experiments, see Supplementary Table 1); and were sorted for DN1 progenitors (Lin- CD45+c-Kit^{hi}CD44^{hi}CD25-) or DN2 progenitors (Lin-CD45+c-Kit^{hi}CD44^{hi}CD25+). DN2 progenitors were further subdivided according to their level of Bcl11b-YFP expression, as indicated (Figs. 2–7), and cells transduced with retrovirus were further isolated as mCherry+ cells (Figs. 6, 7).

For cell proliferation experiments (Fig. 3), sorted cells were further incubated with 5 μM of the CellTrace Violet cell proliferation dye (Invitrogen) at 37°C for 10 minutes prior to culture. The c-Myc retroviral construct was described previously[33]. The small molecule CDK4/6 inhibitor PD0332991 (Selleck Chemicals, Houston, TX) was added to culture medium at a final concentration of 2.1 μM in 0.02% DMSO.[33].

In vitro developmental assays

Thymus or bone-marrow derived DN progenitors were seeded onto monolayers of OP9-GFP or OP9-DL1-GFP feeder cells[30], and cultured in standard media supplemented with 5 ng/ml IL-7, 5 ng/ml FLt3L and 5 μm β-Mercaptoethanol, unless otherwise indicated. In alternate lineage potential assays (Fig. 2a and 2c), a fixed number of cells were deposited by the cell sorter into 96 well plates as indicated; for the other assays, cells were first sorted into tubes, and distributed manually afterwards. Cells were then cultured for the indicated amount of days, then harvested for flow cytometry. For analysis, cells were stained for CD45, CD25 and other antibodies as indicated (Fig. 3, 6 and 7), or with CD11c, NK1.1 and DX5 for

alternate lineage potential assays (Fig. 2). Stained cells were then analyzed using either the MacsQuant flow cytometer (Figs. 3, 5, and Supplementary Fig. 3), or the MacsQuant VYB flow cytometer (Figs. 6, 7, and Supplementary Fig. 5) for detection of mCherry fluorescence by 561nm laser excitation. For feeder-free cultures (Fig. 6), bone marrow-derived progenitors were cultured directly onto DL1 protein coated plates, prepared as a described above, with standard media supplemented with 5 ng/ml SCF, IL-7 and Flt3L, and 5 μM β-mercaptoethanol.

For live imaging, *in vitro* developmental assays were modified in two ways: Firstly, non-GFP expressing OP9 cells (either OP9 parental cells[48], or OP9-DL1-hCD8 cells generated above) were used, to minimize interference in detection of the Bcl11b-YFP fluorescence signal. Secondly, we attached PDMS micromesh arrays (250 μm hole diameter, Microsurfaces, AU) to the surface of glass-bottomed 24 well plates (Mattek, Ashland, MA); these arrays contain small microwells that confine OP9 cells and T-cell progenitors to a single imaging field of view on 40× objective (see Supplementary Fig. 4). OP9 cells and sorted progenitors were then seeded into microwells at appropriate densities to enable cell tracking and prevent cell crowding (~8/well and 1/well, respectively).

To facilitate automated cell tracking in movies, cells were marked with constitutively expressed fluorescence markers in two ways: 1) infection with H2B-mCherry expressing retrovirus (FIg. 5A,B,D and E, and Fig. S4B). Here, sorted cells were then seeded onto virus-boated plates, and cultured in standard media with 5 ng/ml SCF, IL-7, and Flt3L. After 8 hours of infection, cells were transferred onto OP9-DL1 monolayers in microwells, and then subject to timelapse live-cell imaging. 2) *in situ* staining with an fluorescence-conjugated antibody to the pan-hematopoietic cell marker CD45. Following a previously described procedure[49], 50 ng/ml of CD45-APC was added to the culture media for imaged cells. In separate experiments, we verified using flow cytometry that direct addition of this antibody to culture media did not affect the T-cell development at these stages (not shown).

Isolation, activation and transduction of peripheral T-cells

To purify peripheral T-cells from spleen, we incubated splenocytes with biotin-conjugated CD4 and CD8 antibodies, followed by streptavidin-coated magnetic beads (Miltenyi Biotec), and passed them through a magnetic column. Trapped $CD4^+$ or $CD8^+$ cells were then eluted, and activated by culture with anti-TCRβ (plate-immobilized, 1 μg/ml coating concentration) and anti-CD28 antibody (in solution, 1 μg/ml) for one day. After activation, cells were transferred onto retronectin and virus-coated plates for retroviral transduction. After three days, cells were resuspended, stained with a fluorescence-conjugated CD8 antibody, and then analyzed using flow cytometry. In these experiments, cells were cultured in lymphocyte media (RPMI medium supplemented with 10% fetal bovine serum, penicillin-streptomycin-glutamine, nonessential amino acids, sodium pyruvate, and 2-mercaptoethanol) supplemented with 100 U/ml IL-2 (Peprotech). Figure 8f,g shows results for $CD8^+$ cells while Supplementary Fig. 8b shows those for $CD8^-$ ($CD4^+$) cells, because CD8 surface levels are more stable under these stimulation conditions.

Statistical analysis of alternate lineage potential

In alternate lineage potential assays, wells seeded with low numbers of starting precursors (input numbers indicated on figure panels) were first scored for NK cell or DC development using flow cytometry, using the markers NK1.1-DX5 for NK cells and CD11c for DC (Fig. 2a, bottom, and 2c). A model, logistic in log of starting cell number, was fit, and the probability of a positive well from 10 cells was taken as a measure of developmental potential. The effect of Bcl11b-YFP activation on developmental potential was estimated as the difference of these probabilities, and tested by comparing the difference to its standard error using a *z*-statistic.

Sample preparation for RNA-Seq

Total RNA was extracted from 1–2.5 million cells using Trizol (Invitrogen), and then subjected to two rounds of selection using Oligo-dT coupled magnetic beads (Dynabeads) according to the manufacturer's protocol. About 50–100 ng polyadenylated mRNA per sample was obtained after double selection. RNA was fragmented to an average length of 200 bp by Mg^{2+}-catalyzed hydrolysis and then converted into cDNA by random priming. cDNA was then subjected to end repairing, adaptor ligation, size selection and one round of PCR amplification.

Analysis of RNA-Seq data

RNA-Seq data was analyzed with an established analysis pipeline consisting of the programs TopHat and Cufflinks[50], and output data were further analyzed and visualized using MATLAB (Natick, MA). Briefly, reads from the sequencer were mapped onto the *mm9* reference genome using the Tophat. Gene expression values, in fragments per kilobase-million (FPKM) were then obtained, and differential expression analysis with replicate biological data was then performed using the statistical model from the Cufflinks software.

For principal component analysis (PCA) of developmental trajectories (Fig. 2D), we first obtained the set of all differentially expressed genes across the ETP (DN1), DN2a and DN2b stages from our previous study[25], using pairwise comparisons with a probabilistic cutoff of $p < 0.002$. FPKM values for these genes from both our past study and this current work were log-transformed and normalized across all conditions, with normalizations being performed separately for these two datasets to prevent non-developmental differences in gene expression from obscuring the PCA analysis. Projections and loadings along the first two principal components were then plotted (Fig. 2d).

For analysis of gene expression changes during Bcl11b activation, we either started with a list of genes that were differentially expressed upon Bcl11b activation ($p < 0.005$, between Bcl11b-YFP^{-} and Bcl11b-YFP^{+} DN2 cells, Fig. 2e left and Supplementary Table 1), or with a manually selected list of regulatory genes known to be important for T-cell development (Fig. 2e right and Supplementary Table 2). Weakly expressed genes with a total count number < 5 were then excluded, and remaining genes were then subject to a hierarchical clustering using an un-weighted average distance metric. Computed clusters were then visualized using heat maps (Fig. 2e).

Retroviral transduction and preparation of the DL1-coated plates

Viral particles were generated by transient co-transfection of the Phoenix-Eco packaging cell line with the retroviral construct and the pCL-Eco plasmid (Imgenex, San Diego, CA). Viral supernatants were harvested at two and three days after transfection, and immediately frozen at -80°C until use. For experiments involving retroviral transduction (Figs. 6–7), tissue culture plates (Costar, Corning) were incubated overnight with 33 μg/ml Retronectin (Clontech) and 2 μg/ml of DL1-ext-IgG protein, and then loaded with viral supernatant. Cells were then cultured directly on virus-bound plates under the conditions described below. For experiments involving culture of sorted progenitors on DL1-coated plates (Fig. 6), tissue culture plates (Costar, Corning) were incubated overnight with 33 μg/ml Retronectin (Clontech) with different concentrations of the DL1-ext-IgG protein, as indicated.

Generation of OP9-DL1-hCD8 cell lines

OP9 cells[48] were transduced with DL1-IRES-hCD8 retrovirus, and single hCD8- expressing cell clones were generated by sorting low, limiting numbers of hCD8+ cells onto 96 well plates. Individual clones of OP9-DL1-hCD8 infected cells were then assayed for their ability to support T-cell development and survival, and working clones were then expanded, frozen and used for subsequent experiments.

Live-cell imaging

Long-term timelapse imaging of cultured tells was performed using a previously described method with some modifications[33]. Briefly, imaging was performed on a motorized inverted fluorescence microscope (IX-81, Olympus) using a 40× 0.95 NA oil objective (Supplementary Fig. 4). The microscope was fitted with laser-based focus drift correction (ZDC, Olympus) to maintain a constant plane of imaging, and also fitted with a custom-built incubator to maintain a constant humidified environment at 37°C with 7% CO_2. Images of cultured cells were acquired at fixed time intervals in the differential interference contrast (DIC), YFP, and mCherry or APC channels using image acquisition software (Metamorph, Molecular Devices). Shorter timelapse intervals (3 minutes) were for DIC image acquisition, whereas longer timelapse intervals (15 minutes) were used for acquisition of fluorescence images to minimize photo-toxicity. At each time interval, multiple microwells within the microwell array were visited using a motorized X-Y stage (ASI Scientific). To correct for uneven fluorescence illumination, tiled images of uniformly fluorescent beads (Tetraspeck beads, Invitrogen) were acquired in the same fluorescence channels, and processed to generate a correction matrix, as previously described[33].

Image segmentation and analysis

Cells were segmented and tracked using custom image processing workflow implemented in MATLAB (Mathworks, Natick, MA), which we previously described in detail[33]. Briefly, this workflow involved the following steps: Firstly, images were corrected for uneven illumination correction and background-subtracted. A matrix for correcting uneven illumination was calculated from fluorescent bead images, and applied to the fluorescence images. Corrected images were then subtracted for background using a top-hat filter.

Secondly, cells were subject to automated segmentation. Images were smoothed using Gaussian filtering, run through a Laplacian filter to detect fluorescence object boundaries, and thresholded. Resultant closed object boundaries were then filled to generate solid segmented objects, and then subject to size and shape selection to identify cells. Thirdly, cells were tracked automatically. Objects from adjacent movie frames were matched using the Munkres assignment algorithm, using an objective function that incorporates differences in Euclidean distance, shape and object brightness. This automated tracking procedure generates many cell tracking, which are subsequently corrected using supervised methods, as described below. Fourthly, cell segmentation and tracking. Cells that were then automatically segmented and tracked were then subject to manual refinement to identify missed cells, split touching cells, and label cell division events. For one of the imaging data sets (data in Fig. 5a, b, d, e), we performed manual refinement on cell segmentation, but did not further refine automated cell tracking results, nor did we further utilize tracking information for subsequent analysis. To expedite these corrections, we developed a MATLAB graphical user interface that allows a user to review and edit objects and tracks from a timelapse movie. Image analysis code is available upon request from H.Y.K.

Supplementary Material

Refer to Web version on PubMed Central for supplementary material.

Acknowledgments

We thank M. Lerica Gutierrez Quiloan for assistance with mouse genotyping and maintenance; N. Verduzco and I. Soto for animal husbandry; J. Longmate for help with statistical analysis of alternate lineage potential experiments; S. Diamond, K. Beadle, J. Grimm, D. Perez and J. Verceles for cell sorting; N. Feng for initial flow cytometric analysis; J. Hahn for advice on BAC recombineering; S. Qin for assistance with qPCR experiments; X. Wang for performing pilot studies with microwell arrays; and J. Ungerbäck for assistance with visualizing genome track data. We also thank A. Bhandoola, L. Xu and W. Pear (Department of Pathology & Laboratory Medicine, University of Pennsylvania), J. Telfer (Veterinary & Animal Sciences, U. Massachusetts Amherst), and N. Masuyama (Institute of Molecular and Cellular Biosciences, University of Tokyo) for constructs. This work was funded by a CRI/Irvington Postdoctoral Fellowship and an NIH K99/R00 Award (K99HL119638A) to H.Y.K.; a California Institute for Regenerative Medicine Bridges to Stem-Cell Research award to K.K.H.N.; NIH grants to E.V.R. (R01 AI083514, R01 AI095943, RC2 CA148278, R33 HL089123, R01 CA90233 and R01 HL119102) and M.A.Y. (R01 AI064590); the Albert Billings Ruddock Professorship to E.V.R., the Al Sherman Foundation, and the Louis A. Garfinkle Memorial Laboratory Fund.

Reference List

1. Rothenberg EV. T cell lineage commitment: identity and renunciation. J Immunol. 2011; 186:6649–6655. [PubMed: 21646301]
2. Yui MA, Rothenberg EV. Developmental gene networks: a triathlon on the course to T cell identity. Nat Rev Immunol. 2014; 14:529–545. [PubMed: 25060579]
3. Avram D, Califano D. The multifaceted roles of Bcl11b in thymic and peripheral T cells: impact on immune diseases. J Immunol. 2014; 193:2059–2065. [PubMed: 25128552]
4. Ciofani M, et al. A validated regulatory network for Th17 cell specification. Cell. 2012; 151:289–303. [PubMed: 23021777]
5. Liu P, Li P, Burke S. Critical roles of Bcl11b in T-cell development and maintenance of T-cell identity. Immunol Rev. 2010; 238:138–149. [PubMed: 20969590]
6. Li L, Leid M, Rothenberg EV. An early T cell lineage commitment checkpoint dependent on the transcription factor Bcl11b. Science. 2010; 329:89–93. [PubMed: 20595614]

7. Ikawa T, et al. An essential developmental checkpoint for production of the T cell lineage. Science. 2010; 329:93–96. [PubMed: 20595615]
8. Wakabayashi Y, et al. Bcl11b is required for differentiation and survival of αβ T lymphocytes. Nat Immunol. 2003; 4:533–539. [PubMed: 12717433]
9. Inoue J, et al. Expression of TCRαβ partly rescues developmental arrest and apoptosis of αβ T cells in Bcl11b$^{-/-}$ mice. J Immunol. 2006; 176:5871–5879. [PubMed: 16670294]
10. Li P, et al. Reprogramming of T cells to natural killer-like cells upon Bcl11b deletion. Science. 2010; 329:85–89. [PubMed: 20538915]
11. Yui MA, Feng N, Rothenberg EV. Fine-scale staging of T cell lineage commitment in adult mouse thymus. J Immunol. 2010; 185:284–293. [PubMed: 20543111]
12. Naito T, Tanaka H, Naoe Y, Taniuchi I. Transcriptional control of T-cell development. Int Immunol. 2011; 23:661–668. [PubMed: 21948191]
13. Manesso E, Chickarmane V, Kueh HY, Rothenberg EV, Peterson C. Computational modelling of T-cell formation kinetics: output regulated by initial proliferation-linked deferral of developmental competence. J R Soc Interface. 2013; 10:20120774. [PubMed: 23152106]
14. Guo Y, Maillard I, Chakraborti S, Rothenberg EV, Speck NA. Core binding factors are necessary for natural killer cell development and cooperate with Notch signaling during T-cell specification. Blood. 2008; 112:480–492. [PubMed: 18390836]
15. Weber BN, et al. A critical role for TCF-1 in T-lineage specification and differentiation. Nature. 2011; 476:63–68. [PubMed: 21814277]
16. García-Ojeda ME, et al. GATA-3 promotes T-cell specification by repressing B-cell potential in pro-T cells in mice. Blood. 2013; 121:1749–1759. [PubMed: 23287858]
17. Scripture-Adams DD, et al. GATA-3 dose-dependent checkpoints in early T cell commitment. J Immunol. 2014; 193:3470–3491. [PubMed: 25172496]
18. Franco CB, et al. Notch/Delta signaling constrains reengineering of pro-T cells by PU.1. Proc Natl Acad Sci U S A. 2006; 103:11993–11998. [PubMed: 16880393]
19. Germar K, et al. T-cell factor 1 is a gatekeeper for T-cell specification in response to Notch signaling. Proc Natl Acad Sci U S A. 2011; 108:20060–20065. [PubMed: 22109558]
20. Del Real MM, Rothenberg EV. Architecture of a lymphomyeloid developmental switch controlled by PU.1, Notch and Gata3. Development. 2013; 140:1207–1219. [PubMed: 23444353]
21. Panne D. The enhanceosome. Curr Opin Struct Biol. 2008; 18:236–242. [PubMed: 18206362]
22. Spitz F, Furlong EE. Transcription factors: from enhancer binding to developmental control. Nat Rev Genet. 2012; 13:613–626. [PubMed: 22868264]
23. Iwafuchi-Doi M, Zaret KS. Pioneer transcription factors in cell reprogramming. Genes Dev. 2014; 28:2679–2692. [PubMed: 25512556]
24. Zhang DX, Glass CK. Towards an understanding of cell-specific functions of signal-dependent transcription factors. J Mol Endocrinol. 2013; 51:T37–T50. [PubMed: 24130129]
25. Zhang JA, Mortazavi A, Williams BA, Wold BJ, Rothenberg EV. Dynamic transformations of genome-wide epigenetic marking and transcriptional control establish T cell identity. Cell. 2012; 149:467–482. [PubMed: 22500808]
26. Wang H, et al. NOTCH1-RBPJ complexes drive target gene expression through dynamic interactions with superenhancers. Proc Natl Acad Sci U S A. 2014; 111:705–710. [PubMed: 24374627]
27. Li L, et al. A far downstream enhancer for murine Bcl11b controls its T-cell specific expression. Blood. 2013; 122:902–911. [PubMed: 23741008]
28. Tydell CC, et al. Molecular dissection of prethymic progenitor entry into the T lymphocyte developmental pathway. J Immunol. 2007; 179:421–438. [PubMed: 17579063]
29. Mingueneau M, et al. The transcriptional landscape of αβ T cell differentiation. Nat Immunol. 2013; 14:619–632. [PubMed: 23644507]
30. Schmitt TM, Zuniga-Pflucker JC. Induction of T cell development from hematopoietic progenitor cells by delta-like-1 in vitro. Immunity. 2002; 17:749–756. [PubMed: 12479821]
31. De Obaldia ME, Bhandoola A. Transcriptional regulation of innate and adaptive lymphocyte lineages. Annu Rev Immunol. 2015; 33:607–642. [PubMed: 25665079]

32. Weng AP, et al. c-Myc is an important direct target of Notch1 in T-cell acute lymphoblastic leukemia/lymphoma. Genes Dev. 2006; 20:2096–2109. [PubMed: 16847353]
33. Kueh HY, Champhekar A, Nutt SL, Elowitz MB, Rothenberg EV. Positive feedback between PU.1 and the cell cycle controls myeloid differentiation. Science. 2013; 341:670–673. [PubMed: 23868921]
34. Varnum-Finney B, et al. Immobilization of Notch ligand, Delta-1, is required for induction of Notch signaling. J Cell Sci. 2000; 113(Pt 23):4313–4318. [PubMed: 11069775]
35. Schmitt TM, Ciofani M, Petrie HT, Zúñiga-Pflücker JC. Maintenance of T cell specification and differentiation requires recurrent Notch receptor-ligand interactions. J Exp Med. 2004; 200:469–479. [PubMed: 15314075]
36. Taghon TN, David ES, Zúñiga-Pflücker JC, Rothenberg EV. Delayed, asynchronous, and reversible T-lineage specification induced by Notch/Delta signaling. Genes Dev. 2005; 19:965–978. [PubMed: 15833919]
37. Hosokawa H, et al. Gata3/Ruvbl2 complex regulates T helper 2 cell proliferation via repression of Cdkn2c expression. Proc Natl Acad Sci U S A. 2013; 110:18626–18631. [PubMed: 24167278]
38. Yu S, et al. The TCF-1 and LEF-1 transcription factors have cooperative and opposing roles in T cell development and malignancy. Immunity. 2012; 37:813–826. [PubMed: 23103132]
39. Kawazu M, et al. Functional domains of Runx1 are differentially required for CD4 repression, TCRβ expression, and CD4/8 double-negative to CD4/8 double-positive transition in thymocyte development. J Immunol. 2005; 174:3526–3533. [PubMed: 15749889]
40. Zarnegar MA, Chen J, Rothenberg EV. Cell-type-specific activation and repression of PU.1 by a complex of discrete, functionally specialized cis-regulatory elements. Mol Cell Biol. 2010; 30:4922–4939. [PubMed: 20696839]
41. Peter, IS.; Davidson, EH. Genomic Control Process: Development and Evolution. Vol. 460. Academic Press; 2015.
42. Takahashi K, Yamanaka S. Induction of pluripotent stem cells from mouse embryonic and adult fibroblast cultures by defined factors. Cell. 2006; 126:663–676. [PubMed: 16904174]
43. Ebina W, Rossi DJ. Transcription factor-mediated reprogramming toward hematopoietic stem cells. EMBO J. 2015; 34:694–709. [PubMed: 25712209]

METHODS-ONLY REFERENCES

44. Liu P, Jenkins NA, Copeland NG. A highly efficient recombineering-based method for generating conditional knockout mutations. Genome Res. 2003; 13:476–484. [PubMed: 12618378]
45. Hernandez-Hoyos G, Anderson MK, Wang C, Rothenberg EV, Alberola-Ila J. GATA-3 expression is controlled by TCR signals and regulates CD4/CD8 differentiation. Immunity. 2003; 19:83–94. [PubMed: 12871641]
46. Telfer JC, Hedblom EE, Anderson MK, Laurent MN, Rothenberg EV. Localization of the domains in Runx transcription factors required for the repression of CD4 in thymocytes. J Immunol. 2004; 172:4359–4370. [PubMed: 15034051]
47. Champhekar A, et al. Regulation of early T-lineage gene expression and developmental progression by the progenitor cell transcription factor PU.1. Genes Dev. 2015; 29:832–848. [PubMed: 25846797]
48. Nakano T, Kodama H, Honjo T. Generation of lymphohematopoietic cells from embryonic stem cells in culture. Science. 1994; 265:1098–1101. [PubMed: 8066449]
49. Schroeder T. Long-term single-cell imaging of mammalian stem cells. Nat Methods. 2011; 8:S30–S35. [PubMed: 21451514]
50. Trapnell C, et al. Differential gene and transcript expression analysis of RNA-seq experiments with TopHat and Cufflinks. Nat Protoc. 2012; 7:562–578. [PubMed: 22383036]

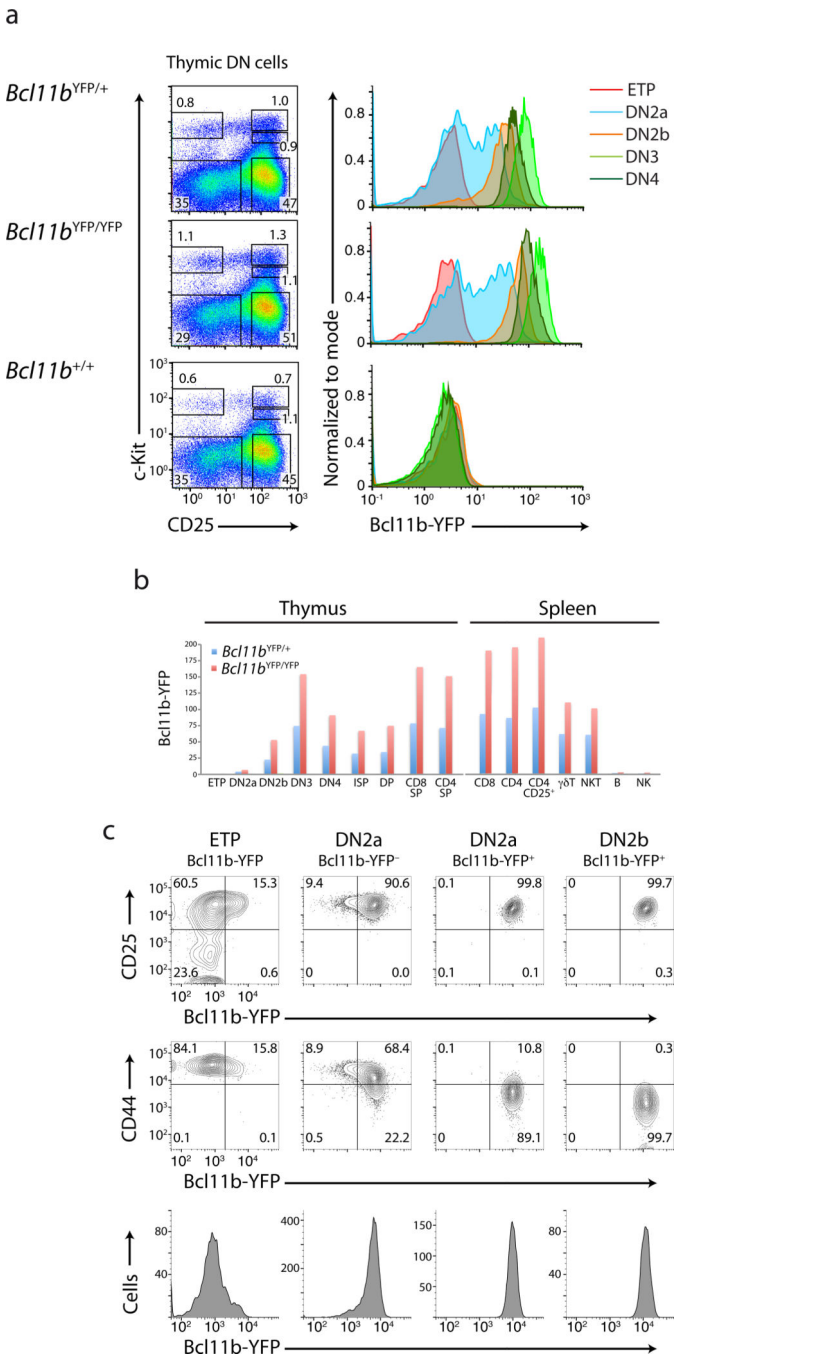

Figure 1. Bcl11b expression turns on in developing T-cell progenitors, and stays on throughout development and maturation

a) Flow cytometry analysis of Bcl11b-YFP levels in CD4, CD8 double negative (DN) thymocytes from single mice containing one, two or zero copies of the Bcl11b-YFP reporter allele, showing gates used for defining DN sub-populations (left), and Bcl11b-YFP level distributions for those populations (right). b) Mean Bcl11b-YFP levels from flow cytometry measurements in various T-cell populations from the thymus (left) or spleen (right) in Bcl11b-YFP reporter mice. Baseline levels in B cells and natural killer (NK) cells, both of which of which do not express Bcl11b, do not exceed 2.6 on this scale, similar to that of T

cells from control C57Bl/6 mice. c) Flow cytometry analysis of T-cell developmental progression and Bcl11b-YFP levels in sorted DN progenitors, cultured for three days on OP9-DL1 monolayers with 5 ng/ml IL-7 and Flt3L. Data are representative of two independent experiments (**a,b**), or three independent experiments (**c**).

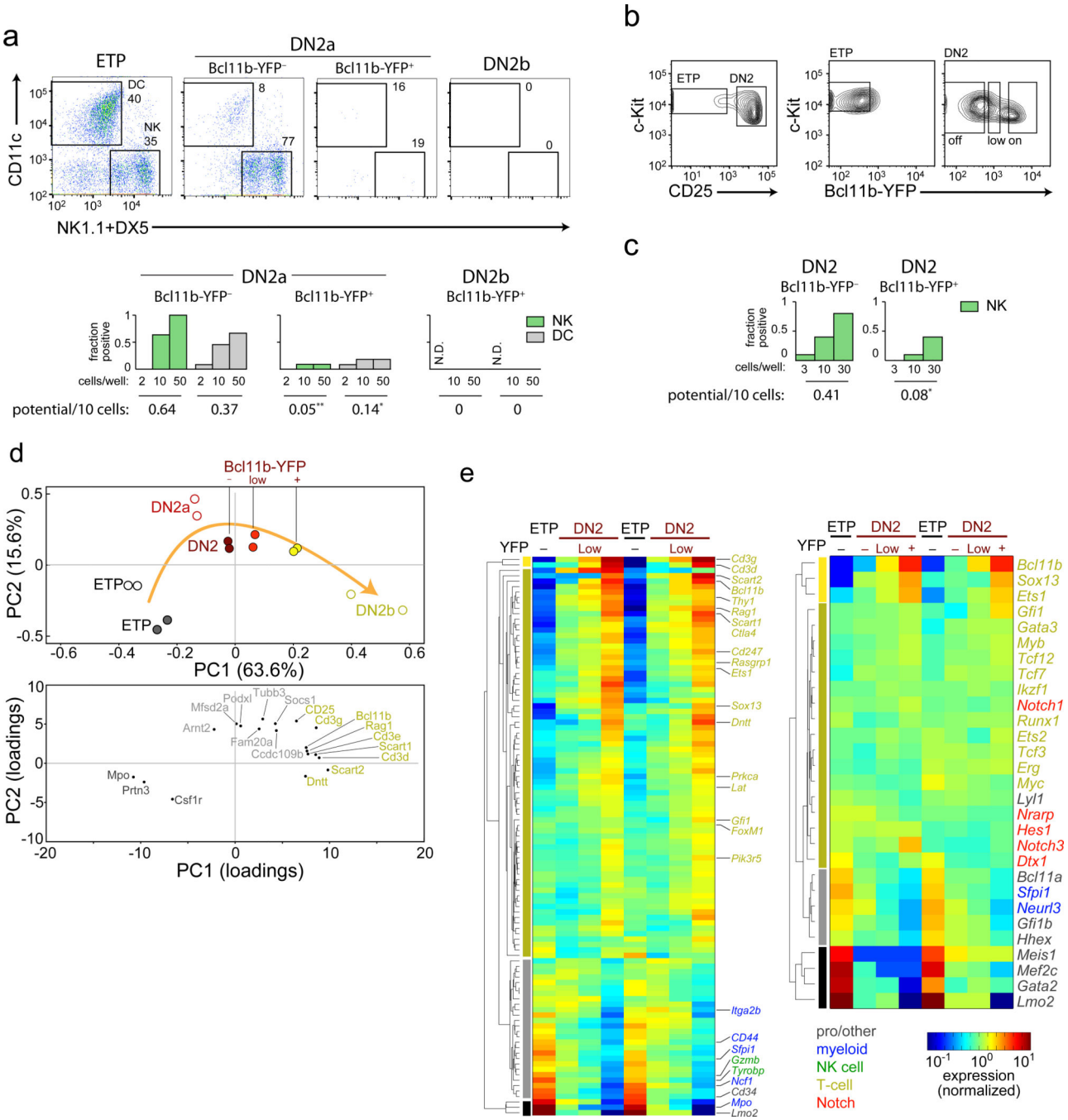

Figure 2. Bcl11b activation coincides with T-cell commitment

a) Analysis of dendritic cell (DC, CD11c$^+$) or NK cell (NK1.1$^+$ or DX5$^+$, mixed antibodies) potential in thymic DN progenitors, assayed after 7–8 days on OP9 monolayers with IL-7 and Flt3L. Wells were seeded with 300 cells (top), or the number indicated (bottom). Bars: fraction of wells with DC or NK progeny for the given number of seeded cells, and inferred lineage potential. Reduced NK and DC potentials between Bcl11b-YFP$^-$DN2 and Bcl11b-YFP$^+$DN2 cells are significant (* - $p = 0.01$; ** - $p = 0.002$; z-test on logistic fit). b)-f) Transcriptomic analysis of bone-marrow DN2 progenitors using RNA-Seq. b) Sort strategy;

c) Analysis of developmental potential in bone-marrow DN progenitors by limiting dilution assays, showing less NK potential in Bcl11b-YFP^{+}DN2 than in Bcl11b-YFP^{-}DN2 (* - p = 0.01; z-test on logistic fit). d) Principal component (PC) analysis (solid circles), showing projections along first two PC axes (top), and loadings of the top ten PC genes (bottom). DN populations from our previous study are shown[25] (open circles). Arrow represents T-cell developmental trajectory. e) Hierarchical clustering analysis of the expression of genes differentially expressed in Bcl11b-YFP^{off} and Bcl11b-YFP^{on} DN2 cells (left, $q < 0.005$), and selected T-cell regulatory genes (right). See Supplementary Tables 1 and 2 for FPKM values. Data in (**a**) represent 12, 11, and 12 replicates (for 2, 10 and 50 cells respectively) in one experiment, with similar results for three independent experiments. Data in (**c**) represent 10 replicates in one experiment, with similar results for two independent experiments. Transcriptomic data (**d,e**) represent biological replicates from two experiments.

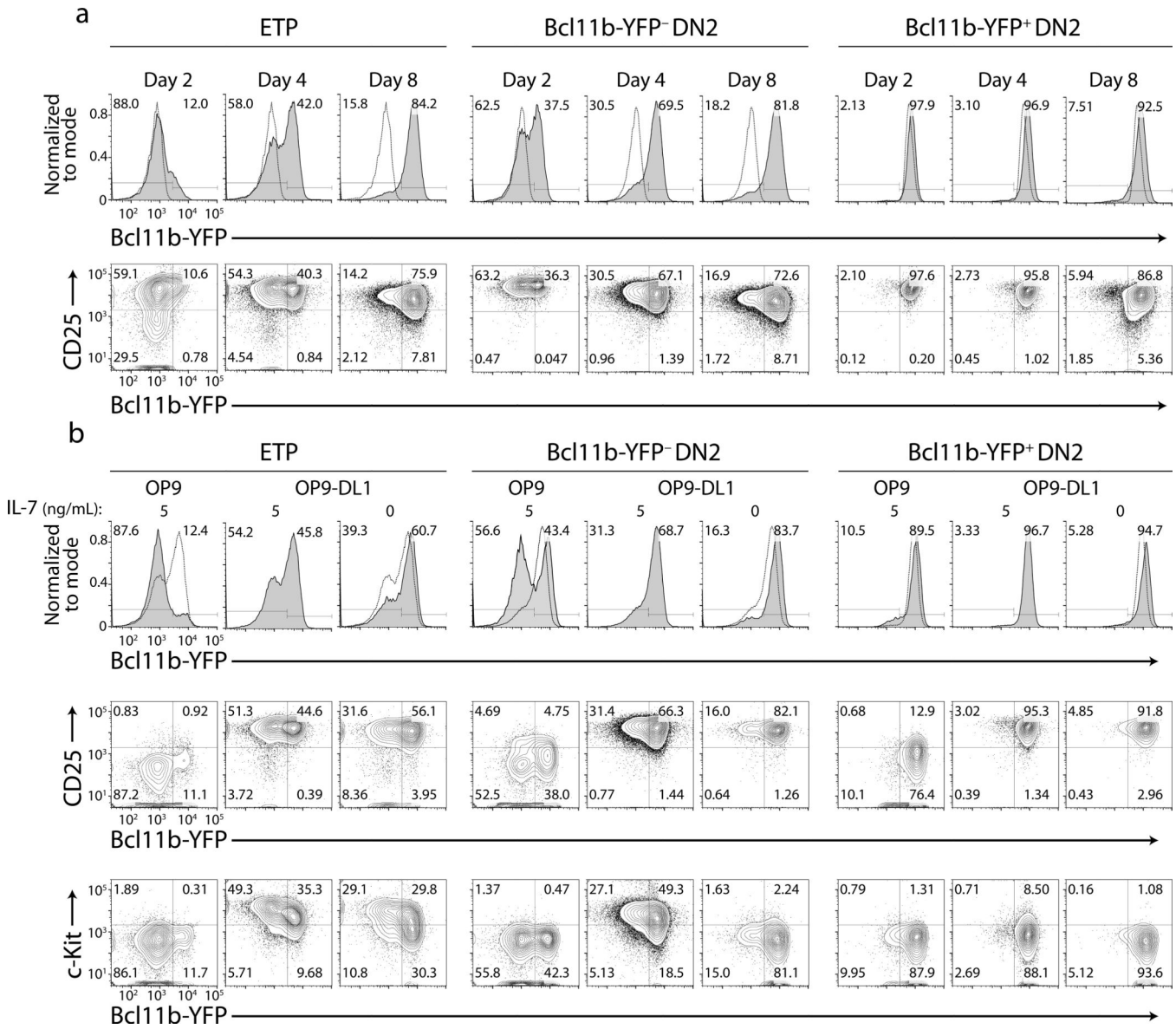

Figure 3. Notch and IL-7 play opposing, stage-specific roles during early T-cell development

a) Flow cytometry analysis of Bcl11b-YFP expression for different BM-derived DN progenitor populations, after culture on OP9 or OP9-DL1 for the indicated number of days. Initial Bcl11b-YFP levels are shown (dotted lines). b) Flow cytometry of different BM-derived DN progenitor populations, after culture under the indicated conditions for 4 days. Results are representative of two (IL-7 titration) or five (Notch withdrawal) independent experiments.

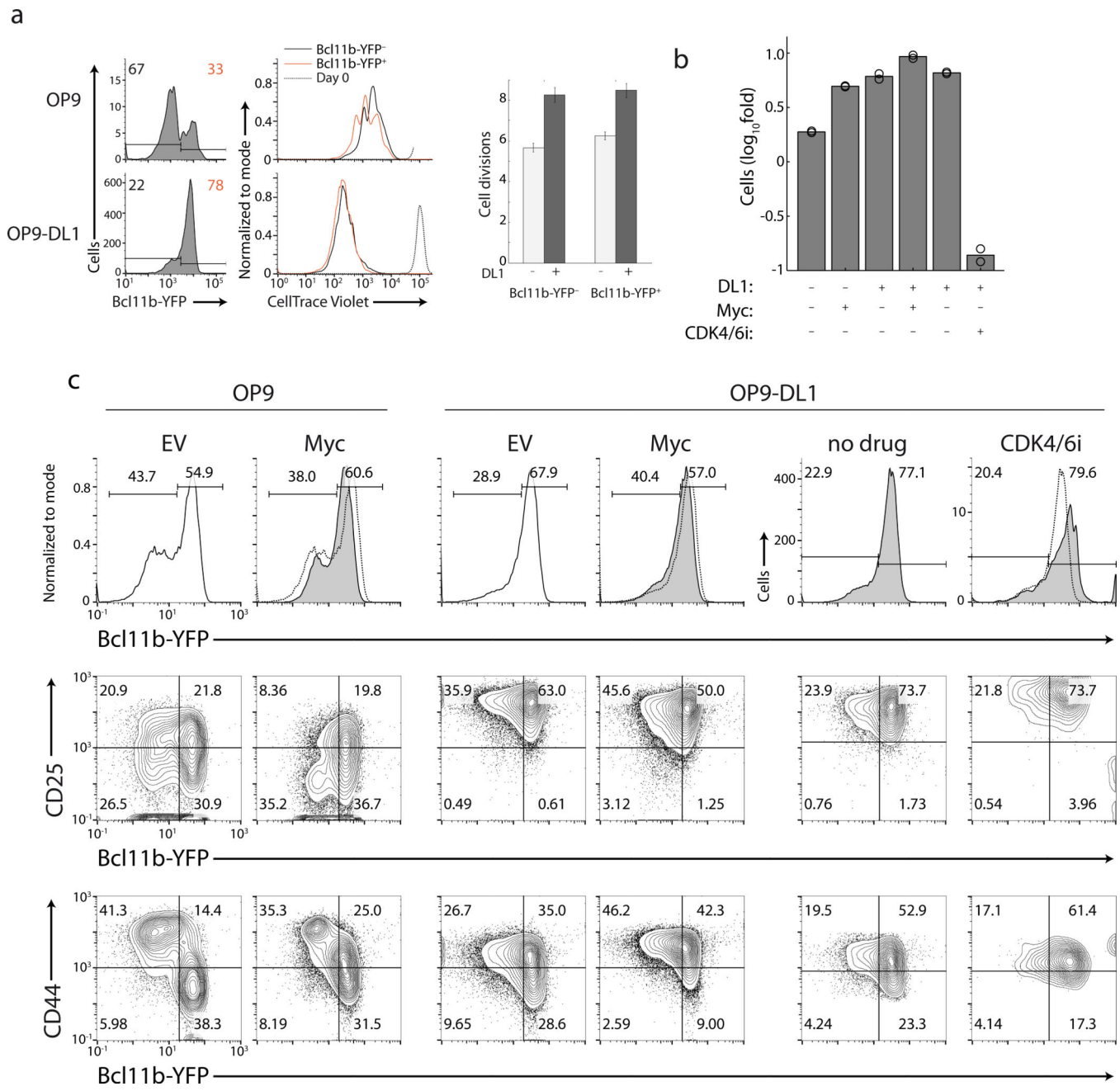

Figure 4. Bcl11b activation is not coupled to Notch-dependent cell proliferation

a) Flow cytometry analysis of Bcl11b expression and cell division kinetics for Bcl11b-YFP⁻DN2 progenitors stained with the cell division dye CellTrace Violet and cultured for four days. CellTrace Violet levels in starting cells are shown (dotted lines). The number of cell divisions is given by the log ratio of initial to final CellTrace Violet levels. b–c) Flow cytometry analysis of BM DN2 progenitors transduced with c-Myc, or treated with the cyclin-dependent kinase (CDK) 4/6 inhibitor PD0332991 (2.1 μM), and analyzed after four days. b) Fold increase in cell numbers under the indicated conditions. c) Analysis of Bcl11b-YFP, CD25 and CD44 expression in the indicated cultured populations. EV – empty vector.

Data in (**a**) represent mean and S.D. of three replicates from one experiment, with similar results seen in independent experiments. Bars in (**b**) represent the mean of two replicates, each shown with circles; results in (**b,c**) are representative of two independent experiments.

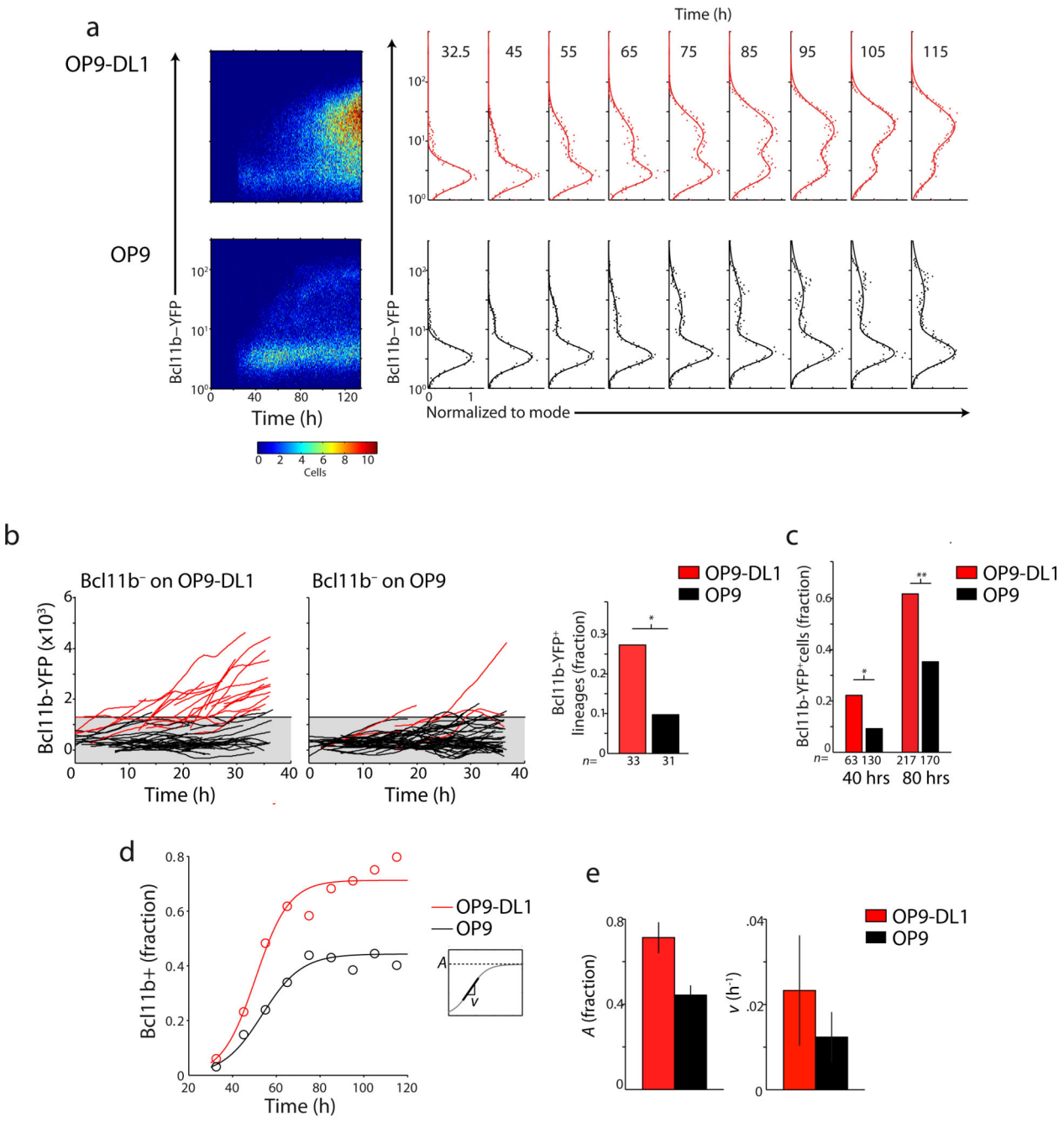

Figure 5. Notch signaling increases the probability of all-or-none Bcl11b activation

a)–d) Long-term timelapse imaging analysis of Bcl11b activation dynamics in single Bcl11b-YFP⁻ DN2 progenitors on OP9 or OP9-DL1 monolayers. a) Time evolution of Bcl11b-YFP levels for a cohort of cells on OP9-DL1 (left, top) or OP9 (left, bottom) monolayers. Histograms (right) give binned cell data obtained at the indicated times (top). Data were shown starting at t~25 hrs onwards, reflecting the onset time for mCherry expression. Smooth lines indicate best fits to mixed Gaussian distributions. b) Single-cell Bcl11b-YFP time traces on OP9-DL1 (left) or OP9 (center) monolayers. Traces where

Bcl11b levels rise above background (gray shading) are indicated in red. Bars give fraction of lineages turning on Bcl11b, showing significant increase in Bcl11b-YFP$^+$ lineages on OP9-DL1 (χ^2=3.25, d.f. = 1; p=0.072). c) Bcl11b-YFP$^+$ cells at 40 and 80 hours, showing significant increase in fraction of Bcl11b-YFP$^+$ cells on OP9-DL1 (40 hrs: χ^2=6.1, d.f. = 1; p=0.013; 80 hrs: χ^2=26.7, d.f. = 1; p=2.4×10^{-7}). d) Time evolution for Bcl11b-YFP$^+$ cells, obtained from Gaussian fits in (**a**). Smooth curves represent fits to the logistic equation $f = A/[1+e^{4\nu(t-\tau)/A}]$. Inset shows graphical depiction of parameters. Bars show initial Bcl11b-YFP activation rate (ν), and maximal fraction of Bcl11b-YFP+ cells (A) from logistic fits, with 95% confidence intervals indicated. Results in (**a,c,d,e**) were obtained from one experiment, and results in (**b**) were obtained from a separate experiment, where cells were tracked to 36 hours. Bar graph data in (**b,c**) were derived from the indicated number of cells (n). Similar results were observed in three independent experiments.

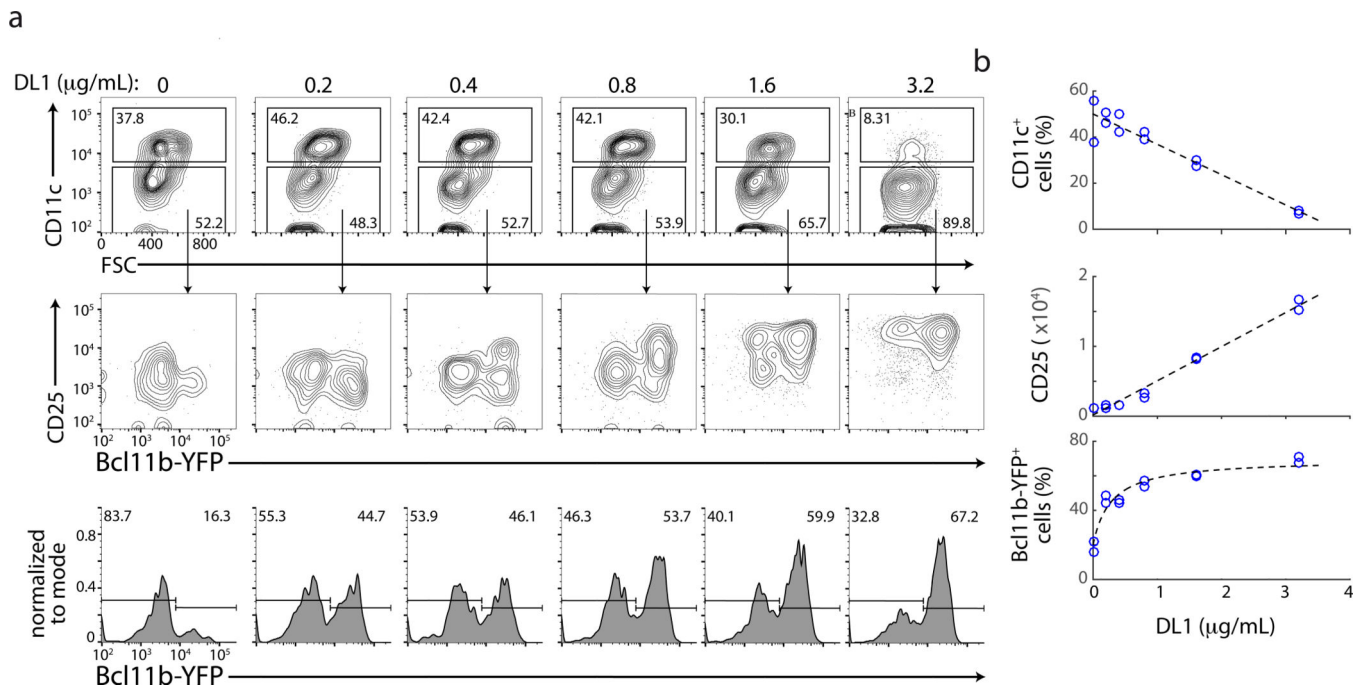

Figure 6. Notch signaling increases Bcl11b activation probability in a dose-dependent manner

a–b) Flow cytometry analysis of BM Bcl11b-YFP$^-$DN2 cells cultured on plates with surface-immobilized DL1 protein, and analyzed after 4 days. a) Levels of the dendritic cell marker CD11c (top), together with CD25 and Bcl11b-YFP levels (middle, bottom) in CD11c- cell populations. B) Percentage of CD11c+ dendritic cells (top), mean CD25 expression levels (center), and Bcl11b-YFP$^+$ percentages (bottom) as a function of DL1 dosage. Curves represent best fit to hyperbolic function $f(x) = x/(x + K_e)$ (bottom), or to a straight line (top, bottom), which was used due to lack of observable saturation in the concentration series. K_e = 0.28 μg/ml represents the DL1 dose required for half-maximal enhancement of Bcl11b activation. FSC - forward scatter. Results are representative of four independent experiments.

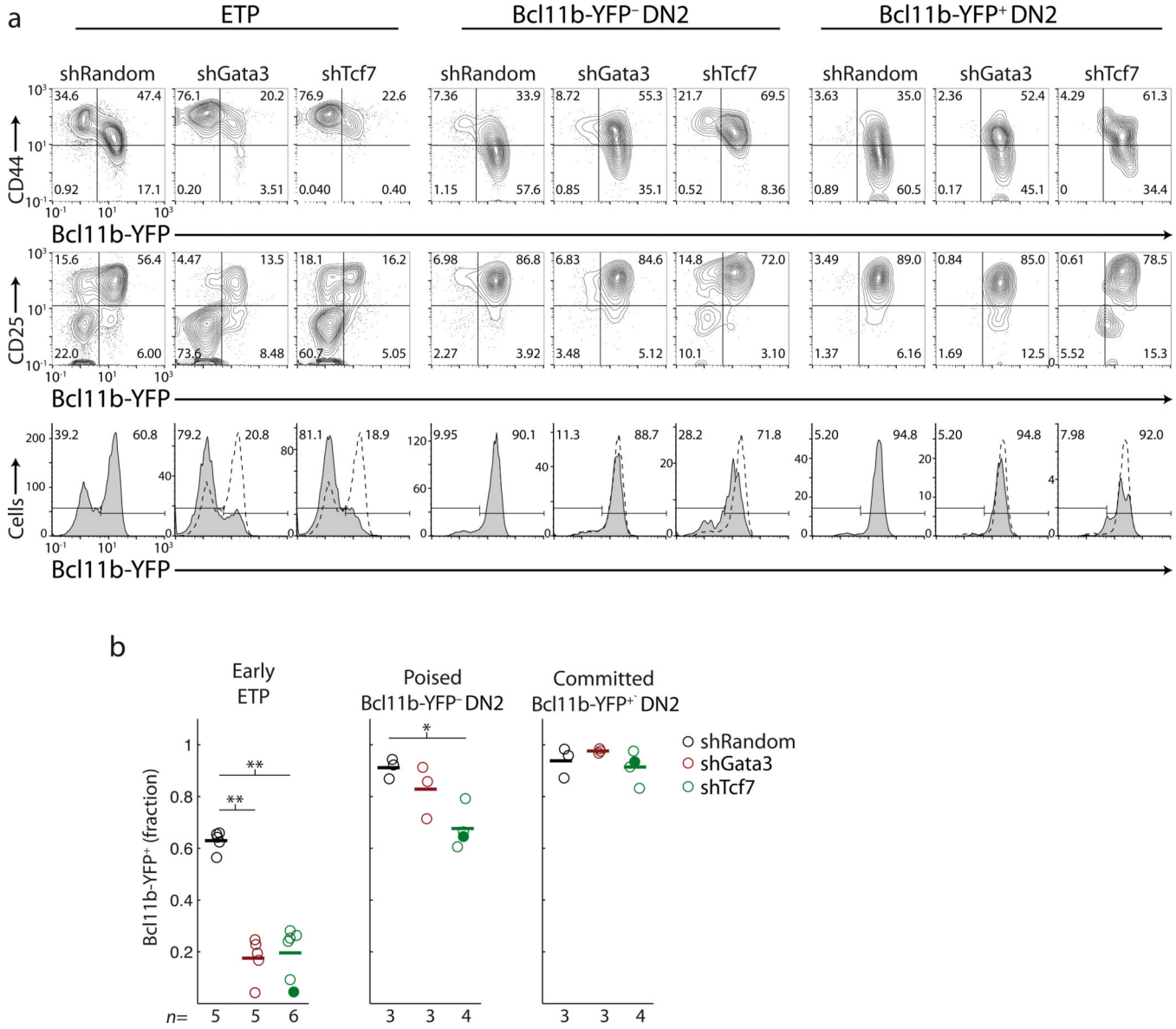

Figure 7. Gata3 and Tcf7 control initial Bcl11b activation

a)–b) Flow cytometry analysis of BM DN progenitors transduced with shRNA to *Gata3* (shGata3) or *Tcf7* (shTcf7), and cultured on OP9-DL1 monolayers with IL-7 and Flt3L for 5–6 days. a) CD44, CD25 and Bcl11b-YFP levels for the indicated cell populations. Cells transduced with non-targeting shRNA sequence (shRandom) are shown with dotted lines. b) Fraction of Bcl11b-YFP$^+$ cells under different conditions. Solid green circles represent data from an alternate *Tcf7* targeting construct (see materials and methods). *Gata3* and *Tcf7* knockdown significantly inhibits Bcl11b activation from ETPs, and in Bcl11b-YFP$^-$DN2 progenitors to a lesser extent (unequal variance *t*-test on perturbed versus control conditions, 1-tailed; * $p < 10^{-2}$; ** - $p < 10^{-4}$), but shows little effect on Bcl11b expression after lineage commitment. Results in (**a**) are representative of two independent experiments, and data in (**b**) show means of the indicated number of replicates (*n*) from two independent experiments.

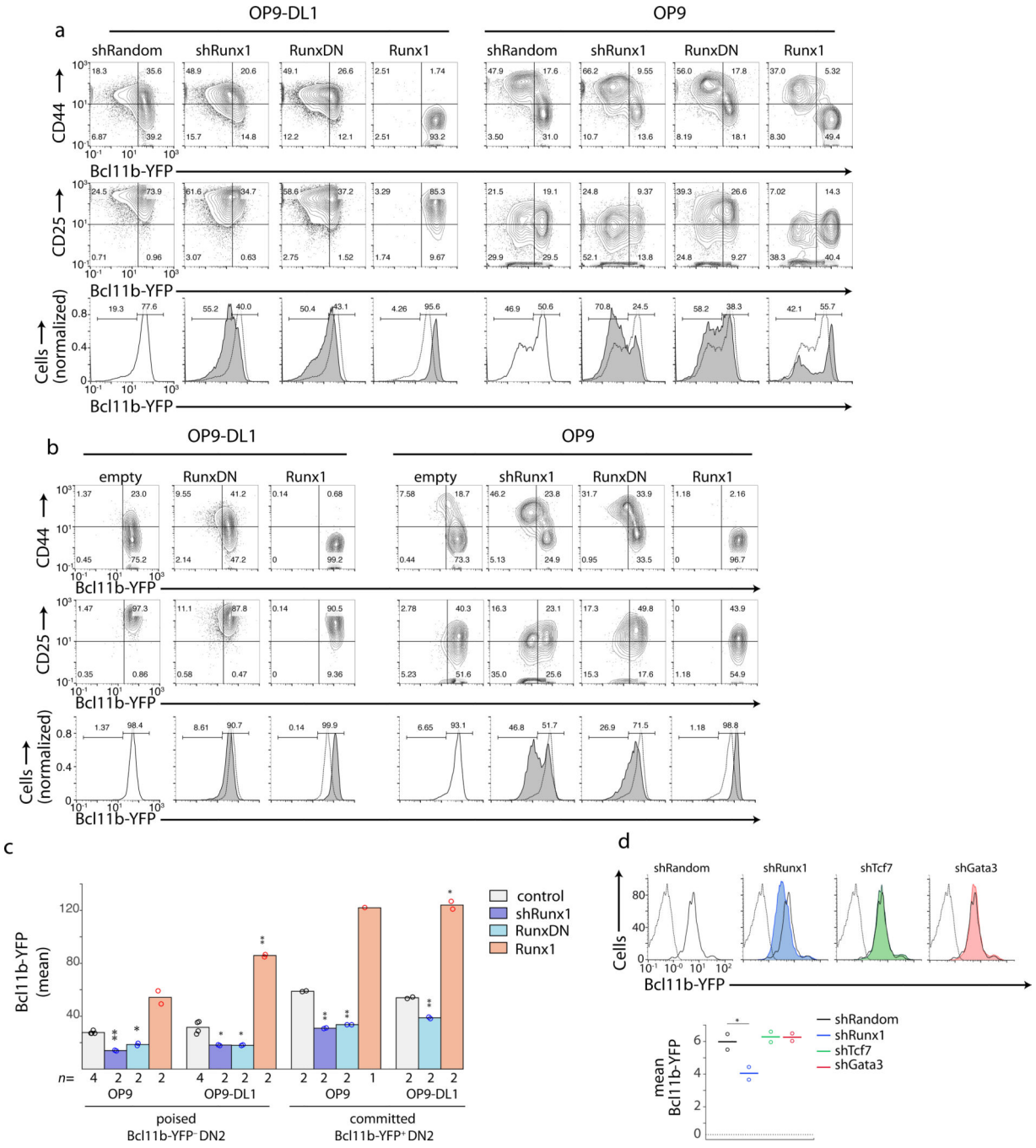

Figure 8. Runx1 controls Bcl11b expression amplitude

a)–b) Flow cytometry analysis of BM DN progenitors transduced with Runx constructs, and cultured on OP9-DL1 or OP9 monolayers for 4 days. CD44, CD25 and Bcl11b-YFP levels are shown for initial Bcl11b-YFP^{-}DN2 cells (**a**) or Bcl11b-YFP^{+}DN2 cells (**b**). shRunx1–*Runx1* shRNA targeting sequence; RunxDN – dominant negative Runx inhibitor; Runx1 – full length *Runx1*; shRandom – non-targeting shRNA sequence; empty – empty vector. In histograms, dotted lines indicate Bcl11b-YFP levels in unperturbed cells. c) Mean Bcl11b-YFP levels under various Runx perturbation conditions. Altering Runx1 levels or activity

significantly alters Bcl1b-YFP levels (unequal variance *t*-test, 2-tailed; * $p < 0.05$; ** - $p < 0.01$). d) Flow cytometry analysis of mature T cells activated with anti-TCRβ and anti-CD28, transduced with the indicated shRNA constructs, and cultured for 3 days. Data shows CD8 T cells (see also Fig. S8). Cells transduced with random shRNA (black solid), and non-fluorescent T cells (black dotted) are shown. Mean Bcl11b-YFP levels decrease significantly upon Runx1 knockdown (unequal variance *t*-test, 1-tailed; * $p < 0.05$). Results in (**a,b**) are representative of two (Runx, shRunx1) or three (RunxDN) independent experiments, and data in (c) represents data and means of the indicated number of replicates (*n*) from one experiment. Data in (**d**) represent means of two replicates from one experiment; results are representative of two independent experiments.